Overview of the Trace Gas Measurements Onboard the Citation Aircraft during the Intensive Field Phase of INDOEX

J.A. de Gouw, H.A. Scheeren, C. Warneke, C. van der Veen, M. Bolder, J. Lelieveld

Institute for Marine and Atmospheric Research, Utrecht University, Utrecht, the Netherlands

M.P. Scheele

Royal Dutch Meteorological Institute, de Bilt, the Netherlands

J. Williams, S. Wong, L. Lange, H. Fischer

Max Planck Institute for Chemistry, Mainz, Germany

Abstract

During the intensive field phase of the Indian Ocean Experiment (INDOEX), measurements of the atmospheric chemical and aerosol composition over the Indian Ocean were performed from a Cessna Citation aircraft. Measurements were performed in February and March 1999, in the part of the Indian Ocean from 70ºE to 80ºE, and from 8ºN to 8ºS in the 0-13 km altitude range. An overview of the trace gas measurements is presented. In the lowest 3 km, the highest levels of pollution were found in the air masses sampled in February 1999, which originated in northeast India, southeast Asia and possibly China. Lower levels of pollution were detected in March 1999, when the sampled air mostly came from the Arabian Sea region. The mixing ratios of a number of trace compounds indicative of biomass burning, were found to be well correlated. The emission factors inferred from the measurements are consistent with literature values for fire plumes, confirming that the residential use of bio-fuels in Asia is a major source of gaseous pollutants to the atmosphere over the Indian Ocean, in accordance with emissions databases. The removal of reactive trace gases could be studied over an extended area without interfering local emissions, and is shown to be governed by photochemical processes. At intermediate altitudes of 3-8 km, the mixing ratios of all trace gases other than ozone were generally lower, and the measurements suggest that the photochemical age of these air masses is longer than in the 0-3 km range. In the 8-13 km altitude range, some evidence is obtained for the importance of convective cloud systems in the transport of gaseous pollutants to the upper troposphere.

Introduction

The goal of the Indian Ocean Experiment (INDOEX) was to characterize and quantify the air pollution emitted in India and southeast Asia, and to study the implications for the global climate and atmospheric composition. In February and March of 1999, during the Intensive Field Phase (IFP) of INDOEX, a Dutch Cessna Citation II research aircraft was operated from the Maldives Islands in the Indian Ocean to measure atmospheric trace gases, aerosols, radiation and cloud droplets. In this paper an overview is given of the trace gas measurements. The Citation aircraft operated in a region south and southwest of the Indian subcontinent from approximately 70°E to 80°E and 8°S to 8°N. During the INDOEX IFP, the meteorology in the region was dominated by the winter monsoon carrying polluted air from India, southeast Asia and possibly China to the measurement area. The inter-tropical convergence zone (ITCZ) was located between 5°S and 12°S. In the lowest atmosphere, the transport and photochemical processing of polluted air could therefore be studied over an extended part of the Indian Ocean without interference from local emissions. Measurements were performed up to altitudes of 13 km, which allowed the upward transport of pollutants to be investigated. It can be expected that pollutants from the lowest atmosphere are efficiently transported to the upper troposphere by the convective cloud systems associated with the ITCZ.

The main finding during the INDOEX IFP was the presence of thick and dense layers of light scattering and absorbing aerosol in the lowest atmosphere north of the ITCZ. The climate implications of these findings have been discussed by Ackerman et al. (2000) and by Satheesh and Ramanathan (2000). Furthermore, it was found that the winter of 1999 saw generally much higher levels of pollution over the Indian Ocean than 1998. The aerosol optical depth observed at the Kaashidoo Climate Observatory (KCO), for instance, had a mean value of 0.41 from January through March of 1999, whereas it was only 0.16 during February and March of 1998 (*Satheesh and Ramanathan*, 2000). Mixing ratios of carbon monoxide (CO) at KCO saw a similar difference between 1998 and 1999 (*Lobert et al.*, 2001). In an INDOEX overview paper, Lelieveld and several co-authors attribute the presence of the aerosol over the Indian Ocean mostly to fossil fuel related emissions, whereas the measurements indicate that the trace gases are mainly released from the residential use of bio-fuels (*Lelieveld et al.*, 2001). The latter conclusion is supported by emissions databases such as EDGAR (=Emissions Database for Global Atmospheric Research), which describes the global emissions of numerous trace gases for several different source categories on a $1^{\circ}\times1^{\circ}$ grid (*Olivier et al.*, 1996).

In this paper, an overview will be presented of the results of the trace gas measurements performed onboard the Citation. We will focus on a number of issues. First, photochemical processing, deposition at the ocean surface and mixing with the free troposphere all lead to removal of trace gases from the lowest 3 km, which is studied here by investigating the north-south gradients in the mixing ratios of the different trace compounds. Second, back-trajectory calculations are used to trace the measured pollution back to its origin. It is found that during February 1999, the air sampled in the lowest 3 km mostly came from the Bay of Bengal carrying high levels of pollution from northeast India, southeast Asia and possibly China. In March 1999, the prevailing wind direction in the lowest 3 km changed from northeast to northwest, bringing less polluted air from the region around the Arabian Sea to the measurement area. Third, the trace gas measurements provide a fingerprint to identify the type of sources responsible for the measured pollutants. According to EDGAR, about 50% of all the anthropogenic carbon dioxide (CO_2) emitted in India is related to the residential use of bio-fuels. Similarly to Lelieveld et al. (2001), the trace gas data from the Citation are therefore compared with data reported in the literature for fire plumes and controlled laboratory burning experiments. Finally, the photochemical age of the sampled air masses, i.e. the time span between sampling and emission at the source, is estimated from the ratio between the concentrations of three different trace gases, which are known to have different photochemical lifetimes in the atmosphere. The analysis gives insight into the dominant atmospheric transport processes which took place in the measurement area.

In this paper, three altitude ranges are considered: (1) 0-3 km, in which the sampled air was directly influenced by emissions in India and Asia, (2) 3-8 km as an intermediate case, and (3) 8-13 km, where trace gas levels were possibly influenced by upward transport of pollutants in convective cloud systems. Furthermore, a simplified data set is used in all of the plots which contains averaged ozone, CO, acetone and acetonitrile mixing ratios for all the level parts of the flights. Along with the averages, standard deviations were calculated, which depend on the precision of the individual data points and on the variability of the mixing ratios during the level flight tracks. Each flight track used consisted of a few minutes of measurement time at least, and therefore at least tens and in some cases up to hundreds of data points were used to obtain the averaged values and standard deviations. The approach improves the measurement precision, in particular of the acetone and acetonitrile data, and enables a direct comparison of the ozone, CO, acetone and acetonitrile data with each other, and with the results of the NMHC data which were obtained from gas chromatographic analyses of canister samples.

More detailed analyses of the data are presented elsewhere in this issue. Warneke et al. describe the results of an experiment in which two consecutive Citation flights were used to study the removal of a number of organic compounds from a certain air mass over the course of one day (*Warneke et al.*, 2001). From the results, a 24-hour averaged OH concentration was calculated, which was shown to be in reasonable agreement with model calculations. Scheeren et al. (2001) focus on the measurements of methyl chloride (CH_3Cl), which proves to be an excellent tracer for the emissions related to bio-fuels. Finally, a case study on the transport of pollutants by convection is presented by Williams et al. (2001).

Aircraft and flight tracks

The measurement flights were performed with a Cessna Citation II twinjet aircraft. The aircraft is jointly owned and operated by the Technical University of Delft and the National Aerospace Laboratory of the Netherlands, and has been used as a platform for atmospheric measurements since 1994. Carrying various payloads, the Citation participated in several measurement campaigns (STREAM, ACE-2, LBA-Claire) to study the chemical and aerosol composition of the atmosphere (*Bregman et al.*, 1995 and 1997; *Fischer et al.*, 1997; *de Reus et al.*, 1998; *Lelieveld et al.*, 1999; *Crutzen et al.*, 2000). The Citation has a maximum altitude of 13 km, a maximum airspeed of 710 km h^{-1} and a flight range of 1100 km at the maximum payload (crew and equipment) of 1400 kg. Flight data (position, wind speed, wind angle, temperature, pressure) are measured continuously, among other using GPS (global positioning system) data.

During INDOEX the scientific payload consisted of several instruments to monitor trace gases, aerosols, radiation and cloud droplets in the atmosphere, in addition to some basic meteorological parameters. Table 1 shows the instruments used for the trace gas measurements. Brief descriptions of the instruments used for the data presented here will be given in the following sections. In addition, measurements of atmospheric particles (number density, size, chemical composition) were performed by Ström and co-workers of the University of Stockholm, Sweden. The light scattering properties were measured by Andreae and a co-worker of the Max Planck Institute for Chemistry in Mainz, Germany. Radiation measurements (j_{NO2}, radial distribution) were done by van Dop, Lelieveld and co-workers of the Institute for Marine and Atmospheric Research of the Utrecht University, the Netherlands. Cloud droplet measurements (FSSP, Gerber) were carried out from March 13th onward by Heymsfield of the National Center for Atmospheric Research (NCAR) in Boulder (Colorado), United States. Apart from the instruments, there was room in the cabin for two operators who ran the different instruments.

In February and March 1999, the Citation was stationed at Male International Airport, on the island of Hulhule in the Republic of Maldives. Figure 1 gives a map of the area and shows the INDOEX flight tracks performed by the Citation. The flight objectives included measurements of background air in the southern hemisphere, pollutant outflow from India and Sri Lanka, pollutant outflow from convective clouds, cloud microphysics, and particle formation at sunrise. Measurement flights were conducted on 16 different days. Fuel stops were made at the island Gan (3 times) in the south of the Maldives and at Colombo Airport on Sri Lanka (1 time).

Meteorology

The meteorology in the area was dominated by the winter monsoon resulting in the transport of pollution from Asia to the region south of the Indian subcontinent where the measurements took place. During most of INDOEX, the ITCZ was located between 5°S and 12°S, i.e. several hundred kilometers south of the Maldives. The outflow of polluted air from Asia could therefore be studied over an extended part of the Indian Ocean. Figure 2 shows a histogram of the wind direction measured onboard the Citation in three different altitude ranges. As expected for the Hadley circulation north of the ITCZ, the winds at low altitudes (0-3 km) were mostly northeast to northwest, whereas at high altitudes (8-13 km) the winds were mostly from the southeast. In the intermediate altitude range of 3-8 km, winds were both from northerly and southerly directions. During INDOEX, the winds in 0-3 km range gradually shifted from northeast in

February 1999 to northwest in March 1999, due to the weakening of the winter monsoon system as a result of the diminishing high pressure over the Indian subcontinent. At high altitudes, there was no obvious difference between the wind directions encountered in February and in March.

A detailed overview of the meteorology in the measurement region is presented elsewhere in this issue (*Verver et al.*, 2001). A few topics which are relevant for the interpretation of the Citation measurements are briefly discussed here. Pollution was advected into a 2-3 km high boundary layer over India and southeast Asia and from there transported towards the south over the Indian Ocean. Over the ocean the boundary layer height generally decreased but an inversion layer at 3 km altitude remained present far from the coast. Far away from the continents a more shallow marine boundary layer of approximately 500 m was found, but this layer was not very clear everywhere. Boundary layer clouds were not very common during the INDOEX IFP, although March 1999 saw somewhat more cloudiness than February 1999. The deep convective cloud systems associated with the ITCZ were mostly too far south to be studied by the Citation. Isolated and small-scale convection was widespread in the measurement area, but generally more in March than in February 1999. The cloud tops of these systems typically reached 10 to 12 km at most and could therefore be investigated by the Citation. The tropopause over the measurement region was much higher than the maximum altitude of the Citation and was approximately 17-18 km during the INDOEX IFP.

Back-trajectories are calculated by Scheele of the Royal Dutch Meteorological Institute (KNMI) for all the level flight tracks of the Citation flights. The KNMI trajectory model uses archived three-dimensional wind data from the European Center for Medium Range Weather Forecasts (ECMWF) model for the calculation of air parcel displacements (*Scheele et al.*, 1996; *Stohl et al.*, 2000). Figure 3 shows the 10-day back-trajectories for all the level flight tracks performed below 3 km (one trajectory per level flight track). During the first part of the INDOEX IFP, the air masses encountered by the Citation were mostly from the Bay of Bengal region and were carrying pollution from northeast India and southeast Asia. On March 4th 1999, the ITCZ was far enough north (1-3°S) for the Citation to reach southern hemispheric air. After March 4, the measured air was mostly from the Arabian Sea and the west coast of India.

As a result of the influence of convection, the back-trajectories calculated for the air masses sampled above 3 km are less reliable: in many cases, slightly different input parameters yield very different back trajectories. The picture that emerges from the trajectory analyses is consistent with the concept of the Hadley circulation north of the ITCZ. In many cases, the air masses sampled in the 8-13 km altitude range came from the southeast and were influenced by convection. The 10-day back trajectories show that these air masses may possibly have come from the direction of southeast Asia, Indonesia, China, and even Australia, but these assignments are highly uncertain. In the intermediate altitude range of 3-8 km, the sampled air masses were influenced by subsidence and to a lesser extent by convection. On February 16th, the air sampled at 7.5 km seems to have come from the atmosphere high above Africa by the jet stream.

Trace gas measurements

Ozone

Ozone (O_3) is one of the most important trace gases in the atmosphere. Its sources in the troposphere include photochemical production involving NO_x (= NO + NO_2), carbon monoxide (CO) and organic compounds, and exchange across the tropopause with ozone-rich air from the stratosphere (*Lelieveld and Dentener*, 2000). Ozone is an important oxidant in the atmosphere: it is the principal precursor of hydroxyl radicals (OH), the reactions of which are the main sink for many different pollutant gases. In addition, ozone is an important greenhouse gas.

The volume mixing ratio (VMR) of ozone was measured continuously onboard the Citation using a commercial chemiluminescence monitor (Bendix 8002), which is based on the reaction between ozone and ethylene (*Bregman et al.*, 1995). The instrument was operated by Scheeren and co-workers of the Institute for Marine and Atmospheric Research of the University of Utrecht in the Netherlands. The instrument was calibrated before and after the campaign, based on the reaction of ozone with a calibrated amount of NO. During the INDOEX IFP, the stability of the instrument's response was checked before and after each flight using an external ozone generator. The overall precision of the instrument is estimated to be ±5%, and the accuracy of the measurement ±10%.

Figure 4 shows the latitude dependence of the ozone VMR observed onboard the Citation. The data shown in Figure 4 (in ppbv = parts per billion by volume) are the averaged values for the level parts of all the flights. The solid symbols represent data taken in February; the open symbols in March 1999. The error bars indicate the standard deviation in the 1s measurements along the level flight parts. For the ozone measurements, the standard deviation is determined by the variability of the ozone VMR along a level flight part. A high standard deviation indicates a strongly variable ozone level, probably caused by the fact that qualitatively different air masses were sampled. It is evident from Figure 4 that in the lower troposphere (0-3 km), there is a clear north-south gradient in the ozone concentration. The full curve shows the result of a least-squares fit of a line to the data (February and March data). The slope is found to be 1.03±0.16 ppbv deg^{-1} latitude, whereas a value of 1.53±0.17 ppbv deg^{-1} latitude is determined for the February data only. In particular the gradient found in the February data is in excellent agreement with the gradients observed during the pre-INDOEX cruise of the research vessel Sagar Kanya: 1.66 ppbv deg^{-1} latitude at 60 ºE, 1.70 ppbv deg^{-1} latitude between 70 and 76 ºE, and 1.35 ppbv deg^{-1} latitude at 76 ºE (*Lal et al.*, 1998). In the intermediate altitude range (3-8 km), there is a similar gradient of 1.2±0.3 ppbv deg^{-1} latitude (February and March data) in the ozone VMR, but it is not as clear as in the 0-3 km altitude range. In the 3-8 km and 8-13 altitude ranges, there is a noticeable difference between the data in February and in March. On a few occasions in February, relatively high ozone VMRs of up to 60 ppbv were observed in the 8-13 km altitude range, possibly as a result of lightning produced NO_x in thunderstorms, or of the intrusion of stratospheric air (*Zachariasse et al.*, 2001). In March, on the other hand, no such high values were observed, and the ozone VMR was found to be relatively independent of latitude in the 8-13 km altitude range.

Figure 5 shows all the data, again averaged per level flight part, vs. the altitude. Again, the error bars show the standard deviation. The scatter in the data at a certain altitude is, among other things, due to the location of the measurement, which is not taken into account in this figure (compare with Figure 4). Nevertheless, it is clear that the ozone VMR increases with altitude. Ozone shows a minimum at low altitudes due to its efficient photochemical loss in the highly humid conditions of the marine boundary layer, and additional removal processes at the ocean surface. At higher altitudes increased ozone concentrations are observed because of (1) in-situ production from lightning-produced NO_x, (2) transport from different areas in the troposphere, and (3) intrusions of stratospheric air. The transport and chemistry involved in determining the ozone above the Indian Ocean will be discussed in detail by Smit et al. in this issue (*Smit et al.*, 2001). The occasionally high ozone values in February at high altitudes are again clear from Figure 5.

In Table 2, average ozone values are given for February and March 1999 in the 3 different altitude ranges. As in Figure 5, it is clear that the ozone mixing ratio increases with altitude. In all three altitude ranges, ozone is slightly lower in March than in February. The presently reported values for ozone in the lowest 3 km (13±5 in February and 12±4 in March 1999) agree well with the mixing ratio of 15.7±2.9 ppbv measured by Rhoads et al. in northern hemisphere continental tropical air over the Indian Ocean in March and April 1995 (*Rhoads et al.*, 1997).

Nitrogen oxides

Nitric oxide (NO) and nitrogen dioxide (NO_2), their sum referred to as NO_x, are among the most important trace gases in the atmosphere. NO_x plays a central role in photochemical ozone production in the troposphere, and is produced both anthropogenically (fossil fuel combustion, biomass burning) and naturally (soils, lightning). During INDOEX, NO was measured onboard the Citation by Lange and co-workers from the Max Planck Institute for Chemistry in Mainz, Germany, using a chemiluminescence monitor (Eco-Physics 780 TR) which is based on the reaction between NO and ozone. The mixing ratio of NO was at or below the detection limit (≈110 pptv; parts per trillion by volume) for most of the INDOEX measurements: the atmospheric lifetime of NO_x is less than a day in the lower troposphere, whereas most of the sampled air was older (three days or more). On a total of six Citation flights, lightning-produced NO_x was observed at high altitudes, where the lifetime of NO_x is significantly higher (up to a week in the upper troposphere).

Carbon monoxide

Carbon monoxide (CO) is an important trace gas in the atmosphere. It is emitted from incomplete combustion such as biomass burning and, to a lesser extent, from the oceans. CO is also formed in the atmosphere from photo-oxidation of methane and higher hydrocarbons. In the remote troposphere, the reaction between CO and hydroxyl radicals (OH) is the main sink for both CO and OH, determining in large part the oxidizing capacity of the background troposphere.

A tunable diode laser absorption spectrometer (TDLAS) was used onboard the Citation to determine ambient CO mixing ratios. These measurements were performed by Fischer and co-workers from the Max Planck Institute for Chemistry in Mainz, Germany. The system applied is specifically designed for airborne trace gas measurements. CO was detected with an integration period of 1 second, an average precision of ± 3.6% (1σ) and a calibration accuracy of 2.8% during the 23 measurement flights performed during the INDOEX campaign. The instrument design has been described in detail elsewhere (*Wienhold et al.*, 1998).

Figure 6 shows the measured CO mixing ratio vs. the latitude in three different altitude ranges. The data are averaged values for all the level parts of the flights performed by the Citation. The solid symbols represent data from February, the open symbols from March 1999. Due to the precision of the CO measurements, the standard deviation is in most cases indicative of the variability of the CO VMR along a level flight track. Below 3 km, it is clear that in February much higher CO levels were found than in March 1999. The CO mixing ratios are weakly dependent on the latitude. From a fit of a line to the data (February and March), a north-south gradient of 3.9±1.9 ppbv deg^{-1} latitude was determined. Above 3 km, there is hardly any latitude dependence of the observed CO mixing ratios.

The main sink for CO in the lower troposphere is the reaction with OH radicals. In another paper in this issue, Warneke et al. describe the results of a Lagrangian experiment, in which the concentration of OH radicals in the boundary layer was determined from the measured removal of several organic compounds from a certain air mass over the course of one day

(*Warneke et al.*, 2001). In this experiment the removal of CO, as a result of its reaction with OH, was determined to be approximately 9.5 ppbv day^{-1}. The average north-south wind speed encountered during the Citation flights below 3 km was measured to be 3.8±0.5 m s^{-1}, or 2.9±0.4 deg latitude day^{-1}. From this, we would expect the north-south gradient of CO to be around 3.2 ppbv deg^{-1} latitude, in good agreement with the value of 3.9±1.9 ppbv deg^{-1} latitude determined from Figure 6. The observation that the north-south gradient in the CO mixing ratio is consistent with the result of the Lagrangian experiment described by Warneke et al. (2001), suggests that the concentration of OH radicals determined in this work is indeed representative for most of the air masses sampled by the Citation flights. Of course, removal of CO from the lowest atmosphere can also occur by mixing with the free troposphere in which CO is generally lower. This is discussed in detail by Warneke et al. and is believed not to have influenced the estimate of the OH concentration significantly. It can not be ruled out, however, that mixing with cleaner air accounts for some of the CO removal observed in Figure 6. Trace compounds more inert than CO do not show a significant north-south gradient, suggesting that mixing between the lowest 3 km of the atmosphere and the free troposphere may not have been very efficient.

Figure 7 shows the measured CO mixing ratios, averaged per level flight part, as a function of altitude. It can be seen that the concentration decreases with altitude, which is expected since the main source of the CO observed here are emissions in India, China and south-east Asia. There is a weak indication of an increase in the CO concentration at an altitude of 10 km. This could be due to vertical transport by convective clouds, which were common during the INDOEX IFP. The issue of transport by convection will be addressed in another paper in this issue by Williams et al. (2001).

Average mixing ratios for CO measured in February and March in the three altitude ranges are given in Table 2. As in the case of ozone, the measurements in February show higher mixing ratios than those in March. The average value observed in March (150±30 ppbv) is somewhat higher than the mixing ratio of 120.4±9.8 ppbv reported by Rhoads et al. for northern hemispheric continental air over the Indian Ocean in March and April 1995 (*Rhoads et al.*, 1997).

Acetone and acetonitrile

Acetone (CH_3COCH_3) and acetonitrile (CH_3CN) are both emitted from bio-fuel use and were found to be useful tracers during INDOEX. Globally, acetone has important sources in biomass burning and the Earth's vegetation, and can also be formed in the atmosphere from hydrocarbon oxidation (*Singh et al.*, 1994). It is a relatively long-lived trace gas which therefore reaches the upper troposphere where it is photolyzed and may contribute significantly to free radical concentrations (*McKeen et al.*, 1997). Acetonitrile is almost exclusively emitted from biomass burning (*Hamm and Warneck*, 1990). It is a long-lived trace gas, as its reaction with OH, the largest know sink, is slow.

Mixing ratios of acetone and acetonitrile were measured on-line with proton-transfer-reaction mass spectrometry (PTR-MS) by de Gouw and co-workers from the Institute for Marine and Atmospheric Research of the University of Utrecht, the Netherlands. In the PTR-MS, chemical ionization of acetone and acetonitrile is achieved through proton-transfer with H_3O^+ ions in a drift-tube reactor. The product ions, $H^+.CH_3COCH_3$ (59 amu) and $H^+.CH_3CN$ (42 amu), are mass analyzed and detected with a quadrupole mass spectrometer (Balzers 422). A detailed description of the PTR-MS technique has been given by Lindinger and co-workers (*Lindinger et al.*, 1998). The PTR-MS which was used on the Citation, was calibrated before and after the campaign using a standard mixture containing a number of volatile organic compounds (VOCs) in N_2. Moreover, the response of the instrument with respect to a certain VOC mixing ratio can be calculated and is found to be in good agreement with the experimentally determined calibration factors. The precision of the acetone measurement during INDOEX is approximately ±20% and for acetonitrile ±30%. The limited precision is due to the limited count rates of product ions: for acetone and acetonitrile approximately 50 ions per second are produced at a mixing ratio of 1 ppbv. Also, when clean air containing no VOCs is sampled, there are background signals due to impurities in the instrument. These backgrounds were measured on a regular basis during the INDOEX flights by passing the sampled air through a charcoal filter. The background is subtracted from the measured mixing ratios to obtain the atmospheric VMRs. This procedure also limits the precision of the method. We estimate the calibration uncertainty to be ±20%, and therefore the overall accuracy of the 1s PTR-MS measurements to be ±40% for acetone and ±50% for acetonitrile. By averaging the data over the level flight tracks, as is done in this paper, the measurement uncertainties in the data points are reduced.

In Figure 8, the observed acetone and acetonitrile mixing ratios are shown as a function of altitude. The data are averaged values for all the level flight parts. The solid symbols represent the data from February, the open symbols from March 1999. The error bars indicate the standard deviation in the 1s data along each of the level flight tracks. The standard deviation of the measured data is determined in large part by the limited precision of the measurements; the atmospheric variability along the level parts of the flights of these relatively long-lived compounds is expected to be smaller. In the 0-3 km altitude range, the acetone and acetonitrile mixing ratios are strongly enhanced. In background conditions, acetone is typically 300-500 pptv and acetonitrile 100-150 pptv (*Singh et al.*, 1994; *Hamm and Warneck*, 1990). The mixing ratio of acetone in particular was higher in February than in March of 1999. Acetone and acetonitrile are relatively long-lived in the atmosphere: acetone has a mean atmospheric lifetime of a few weeks, whereas acetonitrile is less reactive and has a lifetime of a number of months. Accordingly, the north-south gradients in the VMRs of acetone and acetonitrile in the MBL are small, and are not shown here. The altitude profile of acetonitrile will be discussed in detail by de Laat et al. and compared with model calculations (*de Laat et al.*, 2001). Average mixing ratios of acetone and acetonitrile in February and March for the three altitude ranges are given in Table 2. It can be seen that in all altitude ranges, the mixing ratios in February were higher than in March, although some of the differences are within the error bars.

In PTR-MS, only the masses of the ions produced in the drift-tube reactor are determined and interference from other VOCs has to be considered. Formally, the volume mixing ratios presented in Figure 6 should therefore be regarded as upper limits to the genuine mixing ratios of acetone and acetonitrile. A possible interference at the ion signal corresponding to acetone is propanal (C_2H_5CHO). This compound, however, has a much shorter lifetime in the atmosphere than acetone, and it seems unlikely that propanal contributes significantly to the signal observed for acetone: (1) the propanal emitted or formed above the continent is not likely to reach the measurement area, and (2) the mixing ratios of gas–phase precursors for propanal, such as propane and higher NMHCs, were too small over the ocean to explain a significant production of propanal. We do not know of any possible interference at the ion mass corresponding to acetonitrile. Observation of an even mass usually suggests a nitrogen containing ion. We conclude that possible interferences in our measurements were small and well within the other measurement uncertainties.

Non-methane hydrocarbons

During INDOEX, air samples were collected in electropolished stainless-steel canisters onboard the Citation and were analyzed by Scheeren and co-workers at the Institute for Marine and Atmospheric Research of the University of Utrecht, the Netherlands. Levels of organic trace gases in the samples were measured using a gas chromatograph (GC) (Varian Star 3600 CX) equipped with both a flame-ionization detector (FID) for non-methane hydrocarbons (NMHCs), and an electron-capture detector (ECD) for halocarbons. The method is described in detail by Scheeren et al. elsewhere in this issue (*Scheeren et al.*, 2001).

In Table 2, average mixing ratios are listed for ethane (C_2H_6), propane (C_3H_8), acetylene (C_2H_2), benzene (C_6H_6) and methyl chloride (CH_3Cl). As in the previous cases, the mixing ratios were lower in March than in February 1999 in all three altitude ranges. Other compounds determined from the canister measurements include propene (C_3H_6), butane (i-C_4H_{10} and n-C_4H_{10}), pentane (i-C_5H_{12} and n-C_5H_{12}), toluene (C_7H_8) and isoprene (C_5H_8). These compounds are far more reactive, and the measurements are not listed in Table 2 due to their high variability.

Figure 9 shows the north-south gradient in the mixing ratios of ethane, acetylene and benzene measured in the 0-3 km altitude range. It is seen that the mixing ratios of these three compounds decrease towards the south. The significantly lower values at –6°S correspond to gas samples which were taken in an air mass south of the ITCZ. From the data in Figure 9, average north-south gradients are determined of 24±11 pptv deg^{-1} for ethane, 14±6 pptv deg^{-1} for acetylene, and 4.3±1.6 pptv deg^{-1} for benzene. As in the case of CO, the main loss process for these compounds is the reaction with OH radicals. In the Lagrangian experiment described by Warneke et al. (2001), the loss of these compounds over the course of one day was measured to be 90±40 pptv for ethane, 48±8 pptv for acetylene, and 21±8 pptv for benzene. Using an average north-south wind speed of 2.9±0.4 deg latitude day^{-1}, latitude gradients of 30±14 pptv deg^{-1} for ethane, 16±4 pptv deg^{-1} for acetylene, and 7±3 pptv deg^{-1} for benzene are obtained. These are in agreement with the values obtained from the data in Figure 9. The agreement suggests that the removal of these organic compounds is governed in large part by photochemical processes, and that the concentration of OH radicals in the MBL determined from the Lagrangian experiment is consistent with the whole data set. Of course, mixing with cleaner air from the free troposphere is another mechanism for NMHC removal from the lowest atmosphere, and it can not be ruled out that the measurement results in Figure 9 were influenced by this effect. Due to the large error bars, we feel that no further conclusions should be drawn from this analysis.

No data on the halocarbons are presented here. At present, the accuracy of the data is insufficient for publication due to uncertainties in the calibration standard available in the laboratory in Utrecht. More work is needed to validate the INDOEX results.

Discussion

Source regions

Figure 3 shows the calculated ten-day back-trajectories of all the air masses sampled by the Citation below an altitude of 3 km. The trajectories have been divided in three groups, based on the origin of the different trajectories: the Bay of Bengal (BB), the Arabian Sea (AS), and the southern hemipshere (SH). Figure 10 shows the average mixing ratios of the different trace gases for the three different source regions. The mixing ratios for all the trace gases were the highest when coming from the Bay of Bengal. Some of the air masses from the Bay of Bengal traveled over Sri Lanka or over southern India, but these were not significantly more polluted than those air masses which traveled only over the Ocean. Apparently, most of the air pollution originated in northeast India, Bangladesh, southeast Asia, or further upwind in China. Figure 10 shows that the air coming from the Arabian Sea was less polluted than the air from the Bay of Bengal. The Citation measurements hardly show significant qualitative differences between the air masses coming from the BB and AS regions. Qualitative differences were seen for the case of methyl chloride: air from the BB was more enriched in this compound than air from the AS, as discussed by Scheeren and co-workers (*Scheeren et al.*, 2001). The more detailed MBL measurements onboard the research vessel Ron Brown during INDOEX revealed some qualitative differences, which will be discussed in more detail elsewhere in this issue (*Dickerson et al.*, 2001; *de Laat et al.*, 2001). The air sampled south of the ITCZ by the Citation, finally, was considerably cleaner, as is clear from Figure 10.

Pollution sources

In Figures 11 and 12, the acetone and acetonitrile mixing ratios are plotted against CO. As in the previous plots, the averaged values for level flight tracks are used and the error bars shown in the figures are given by the standard deviation. It is seen that in the case of acetone there is a good correlation ($r = 0.82$), whereas in the case of acetonitrile the correlation is reasonable ($r = 0.58$). The full lines in Figures 11 and 12 represent the results of an orthogonal distance regression (ODR) analysis, i.e. a linear regression in which errors are allowed in both variables (*Bakwin et al.*, 1997). The slopes of the curves are 1.1 ± 0.4 pptv ppbv^{-1} in the case of acetonitrile and 14.0 ± 1.8 pptv ppbv^{-1} in the case of acetone. The concentration ratios are given in Table 3. Carbon monoxide, acetone and acetonitrile are relatively inert in the atmosphere. Assuming that the reaction with OH is the main removal process, the atmospheric lifetimes are estimated to be 19 days for CO, 18 days for acetone, and 180 days for acetonitrile, These estimates are based on the rate coefficients in Table 3 and a 24-hour averaged OH concentration of 3×10^6 molecules cm^{-3}, which is an average of the results from the Lagrangian experiment and the model calculations described by Warneke et al. (2001). These lifetimes are relatively long compared with the photochemical age of the sampled air masses. Therefore, the concentration ratios measured here can be compared directly to emission ratios measured at the source. The measured value for acetonitrile ($\Delta CH_3CN/\Delta CO=1.1\pm0.4$ pptv ppbv^{-1}) compares very well to the ratio of 1.3 (0.4-2.5) pptv ppbv^{-1} which Holzinger et al. determined from burning experiments with savanna grasses (*Holzinger et al.*, 1999). The measured Δacetone/ΔCO ratio of 14.0±1.8 pptv ppbv^{-1} is higher than the value of 5.4 (1.5-11.7) pptv ppbv^{-1} determined by Holzinger et al. for acetone. Singh et al., however, report Δacetone/ΔCO ratios of 25±5 pptv ppbv^{-1} within fire plumes over eastern Canada (*Singh et al.*, 1994). These authors claim that this may be an upper limit because of the formation of acetone from hydrocarbon oxidation that may have occurred within the sampled plumes. The same holds for our measurements. Also, it is mostly unknown how much Δacetone/ΔCO and Δacetonitrile/ΔCO emission ratios differ with the type of fuels and fires (bio-fuel usage as in this work; savanna grass in the work of Holzinger et al.; forest fires in the work of Singh et al.; burning; smoldering).

In Figure 13, the correlation between CO and a number of NMHCs as well as methyl chloride is presented. The CO values shown here are averaged values for the level flight tracks during which the gas canister were sampled. It is seen that there is an excellent correlation between CO on the one hand, and methyl chloride, acetylene and benzene on the other hand. There is a reasonable correlation between CO and ethane, whereas the correlation between CO and propane is poor. For the latter two compounds, however, we expect that other sources apart from bio-fuel usage, e.g. fossil fuel production and use, are also important in this region. The ΔNMHC/ΔCO concentration ratios are determined by calculating an orthogonal distance regression (ODR) for each of the correlation plots in Figure 13, and the results are given in Table 3, along with values for ΔNMHC/ΔCO from the literature. It can be seen that for acetylene, propane and benzene, the measured values are smaller than the literature values. This is not surprising because the age of the sampled air masses was a few days on average, whereas the atmospheric lifetimes of these compounds are similar. The chemical removal of NMHCs from the sampled plumes proceeds therefore at a faster rate than the removal of CO, and the measured concentration ratios are reduced relative to the source. A closer look at the data in Table 3 reveals that $\Delta NMHC/\Delta CO_{mea}/\Delta NMHC/\Delta CO_{lit}$, i.e. the ratio between the measured and literature value for ΔNMHC/ΔCO, is smaller for the more reactive compounds. The $\Delta CH_3CN/\Delta CO$ ratio, for instance, is close to the literature value, whereas the Δbenzene/ΔCO ratio is 4 times smaller than the number from EDGAR.

The use of correlation plots in the above analysis has some limitations. In between sampling and the time of emission the trace gas composition of a certain air mass can be changed by photochemical processes, mixing with cleaner air masses and possibly by heterogeneous processes. The emission factors inferred from the correlation plots may not be good estimates of the actual values. To take into account the effects of transport, mixing and chemistry within the sampled plumes, we are working on direct comparisons between model calculations of the different trace gases discussed here and the measurements. The model used for this analysis is the ECHAM (European Center Hamburg) general circulation climate model coupled to a tropospheric chemistry model which considers background CH_4, CO, NO_x, HO_x and higher hydrocarbon chemistry. Trace gases such as acetonitrile, which are not included in the standard chemistry scheme, are added off-line to the model calculations. The emissions are parameterized according to EDGAR, and the calculated OH values are used to quantify the chemical removal in the sampled plumes. The first results of this work are promising and are shown elsewhere in this issue (*de Laat et al.*, 2001). It is found, for instance, that the model output for acetone is in good quantitative agreement with the measured acetone over the Indian Ocean. This suggests that the emissions estimates for acetone (and acetone precursors) used as input for the model, i.e. from the EDGAR database, are realistic.

Age of the air masses

The age of the air masses sampled by the Citation during INDOEX were estimated from the measured ratio between two trace compounds with different lifetimes in the atmosphere, assuming that the ratio at the source is given by the EDGAR emission profiles for bio-fuel use. For the INDOEX data, we chose to look at the ratio between benzene and ethane on the hand, and acetylene and ethane on the other hand. Ethane is relatively inert and only a small fraction was removed in the sampled air masses (Figure 9). Benzene and acetylene are shorter lived and are removed much more efficiently from a certain air mass depending on the age. We chose not to look at even shorter lived compounds such as the higher alkanes (butane, pentane) or toluene: the atmospheric lifetimes of these compounds is so short that their mixing ratios are small and thus hard to determine precisely over the Indian Ocean. The age of an air mass, Δt, is estimated from:

$$\Delta t = \frac{-1}{(k_A - k_B)[\mathrm{OH}]} \ln\left(\frac{[\mathrm{A}]_t / [\mathrm{B}]_t}{[\mathrm{A}]_0 / [\mathrm{B}]_0} \right), \qquad (1)$$

where $[\mathrm{A}]_t$ and $[\mathrm{B}]_t$ are the measured mixing ratios of compounds A and B, and $[\mathrm{A}]_0/[\mathrm{B}]_0$ is the ratio between the mixing ratios of compounds A and B assumed at the source. For the emission factors $[\mathrm{A}]_0/[\mathrm{B}]_0$ of ethane, benzene and acetylene, we use the values from Table 3, i.e. the emissions are assumed to be caused by the burning of bio-fuels, with the emission factors given by EDGAR. It is assumed that the removal of compounds A and B is only determined by the reaction of A and B with OH radicals with rate coefficients of k_A and k_B (Table 3), respectively. For the concentration of OH radicals, [OH], a 24-hour averaged value of 3×10^6 molecules cm^{-3} is used, which is an average of the results from the Lagrangian experiment and of the model calculations described by Warneke et al. (2001). In Figure 14, the age determined from the acetylene/ethane ratio is plotted against the age from the benzene/ethane ratio. It is clear that the estimate of the air mass age yields reasonable values: the age varies between 4 and 15 days, in good agreement with the expected values from the back-trajectory calculations (Figure 3). Moreover, there is excellent quantitative agreement between the age estimated from the acetylene/ethane and the benzene/ethane ratio. The dotted line shows the one-to-one relationship, whereas the solid line shows the result of a orthogonal distance regression analysis. The slope of the solid line is 1.2±0.2, i.e. equal to 1 within the error bar, and the offset of the fitted line goes through zero within the error bars. Furthermore, we conclude from the agreement that the emission factors which are used for the calculation, i.e. the EDGAR values, are indeed consistent with the findings for the sampled air masses. This gives further support for the presumption that the burning of bio-fuels contributed significantly to the atmospheric pollutants observed over the Indian Ocean during INDOEX.

In Figure 15, the estimated age of the air masses sampled in the lowest 3 km is plotted against the latitude. As expected the age of the air masses increases on average while going towards the south. The full curve shows the result of a linear least-squares fit to the data, and the slope was found to be 0.38±0.10 day deg^{-1} latitude, suggesting an average north-south wind speed of 2.6±0.7 deg latitude day^{-1}. This result compares very well to the average north-south wind speed of 2.9±0.4 deg latitude day^{-1} observed during the flights in the 0-3 km altitude range. Again, we conclude that the age estimate seems to give reasonable results in the lowest 3 km of the atmosphere.

In Figure 16, the estimated age is plotted against altitude. It is clear that there is a maximum in the age vs. altitude at approximately 4-6 km. This is consistent with the expectation that the outflow of convective clouds, the main mechanism to transport young air from the MBL to high altitudes, takes place at altitudes higher than 8 km. The oldest air is found in the intermediate altitude range from 3-8 km, and apparently not strongly influenced by convection. Transport by convection will be discussed in more detail by Williams et al. elsewhere in this issue (*Williams et al.*, 2001). The age determination for air above 3 km is arguably not as reliable as below 3 km: it is less certain what the source regions are for the air sampled at higher altitudes and whether or not they were influenced by biomass burning emissions. In principle, the air at higher altitudes may have been influenced by qualitatively different pollution, leading to erroneous age estimates in our simple analysis.

Finally, using the estimated age of the sampled air masses, the data plotted in Figure 13 can be corrected for photochemical removal within the sampled plumes. The measured mixing ratios have been extrapolated back to the source by taking into account the age, the rate coefficient for the reaction with OH (Table 3), and a 24-hour averaged OH concentration of 3×10^{6} molecules cm^{-3}. The correlation between the corrected data is still good, except in the case of propane, which suggests again that this compound has other significant sources. Again, an orthogonal distance regression is calculated for the correlation between ethane, acetylene, benzene and CO, and the results are given in Table 3. As expected, the corrected numbers agree somewhat better with the literature values than before. The values for Δethane/ΔCO and

Δacetylene/ΔCO now agree within the error bar with the values from EDGAR. The ratio Δbenzene/ΔCO, on the other hand, is still somewhat lower than the literature value.

Conclusions

An overview is given of the trace gas measurements performed onboard the Citation during the INDOEX IFP in February and March 1999. High levels of pollution were observed over the Indian Ocean on a total number of sixteen flight days. The air sampled in February originated in most cases from the region around the Bay of Bengal and was more polluted than the air sampled in March, when northwesterly winds were carrying pollution from the Arabian Sea region to the measurement area. A high degree of correlation was found between a number trace gases which are indicative of biomass burning. The emission factors inferred from the measurements are consistent with literature values for burning experiments in the laboratory and in the field. Strong evidence is thus obtained to support the presumption that the residential use of bio-fuels is among the most significant sources of gaseous pollutants over the Indian Ocean, as indicated by emissions databases. The removal of pollutants from the lowest 3 km of the troposphere could be studied over an extended area, due to the steady northerly winds and the absence of local sources. The measured north-south gradients in the mixing ratios of a number of trace gases suggest that this removal is mostly governed by photochemical processing. The age of the sampled air masses is estimated from the ratios between trace gases with different atmospheric lifetimes, and confirms the dominant atmospheric transport processes: transport by trade winds in the lowest 3 km towards the south, and upward transport by convection to altitudes above 8 km.

Acknowledgements

This work was financially supported by NWO and FOM. The support of the aircraft technicians (Cor Dam, Jaap Quartel, and Kees van Woerkom) and the pilots (Hessel Benedictus, Alwin Kraeger, Bob Mulder, Tjipke van Netten, and Jurrie van Osnabrugge) in preparing, performing and analyzing the flights is gratefully acknowledged.

References

Ackerman, A.S., O.B. Toon, D.E. Stevens, A.J. Heymsfield, V. Ramanathan, and E.J. Welton, Reduction of tropical cloudiness by soot, *Science*, *288*, 1042, 2000.

Atkinson, R., Gas-phase tropospheric chemistry of organic compounds, *J. Phys. Chem. Ref. Data*, Monograph No.2, 1-216, 1994.

Atkinson, R., D.L. Baulch, R.A. Cox, R.F. Hampton Jr., J.A. Kerr, M.J. Rossi, and J. Troe, Evaluated kinetic, photochemical and heterogeneous data for atmospheric chemistry: supplement V, *J. Phys. Chem. Ref. Data*, *26*, 521, 1997.

Bakwin, P.S., D.F. Hurst, P.P. Tans, and J.W. Elkins, Anthropogenic sources of halocarbons, sulfur hexafluoride, carbon monoxide, and methane in the southeastern United States, *J. Geophys. Res.*, *102*, 15915-15925, 1997.

Bregman, A., P.F.J. van Velthoven, F.G. Wienhold, H. Fischer, T. Zenker, A. Waibel, A. Frenzel, F. Arnold, G.W. Harris, M.J.A. Bolder, and J. Lelieveld, Aircraft measurements of O_3, HNO_3, and N_2O in the winter Arctic lower stratosphere during the Stratosphere-Troposphere Experiment by Aircraft Measurements (STREAM), *J. Geophys. Res.*, *100*, 11245, 1995.

Bregman, A., M. van den Broek, K.S. Carslaw, R. Müller, T. Peter, M.P. Scheele, and J. Lelieveld, Ozone depletion in the late winter lower Arctic stratosphere: Observations and model results, *J. Geophys. Res.*, *102*, 10815, 1997.

Crutzen, P.J., J. Williams, U. Pöschl, P. Hoor, H. Fischer, C. Warneke, R. Holzinger, A. Hansel, W. Lindinger, B. Scheeren, and J. Lelieveld, High spatial and temporal resolution measurements of primary organics and their oxidation products over the tropical forests of Surinam, *Atmos. Environ.*, *34*, 1161-1165, 2000.

de Laat, A.T.J., J.A. de Gouw, J. Lelieveld, A. Hansel, Model analysis of trace gas measurements and pollution impact during INDOEX, *J. Geophys. Res.*, this issue, 2001.

de Reus, M., J. Ström, M. Kulmala, L. Pirjola, J. Lelieveld, C. Schiller, and M. Zöger, Airborne aerosol measurements in the tropopause region and the dependence of new particle formation on preexisting particle number concentration, *J. Geophys. Res.*, *103*, 31255, 1998.

Dickerson, R.R., Overview: The cruise of the research vessel Ronald H. Brown during the Indian Ocean Experiment (INDOEX) 1999, *J. Geophys. Res.*, this issue, 2001.

Fischer, H., A.E. Waibel, M. Welling, F.G. Wienhold, T. Zenker, P.J. Crutzen, F. Arnold, V. Bürger, J. Schneider, A. Bregman, J. Lelieveld, and P.C. Siegmund, Observations of high concentrations of total reactive nitrogen (NO_y) and nitric acid (HNO_3) in the lower Arctic stratosphere during the Stratosphere-Troposphere Experiment by Aircraft Measurements (STREAM) II campaign in February 1995 , *J. Geophys. Res.*, *102*, 23559, 1997.

Hamm, S., and P. Warneck, The interhemispheric distribution and the budget of acetonitrile in the troposphere, *J. Geophys. Res.*, *95*, 20593-20606, 1990.

Holzinger, R., C. Warneke, A. Hansel, A. Jordan, W. Lindinger, D.H. Scharffe, G. Schade, and P.J. Crutzen, Biomass burning as a source of formladehyde, acetaldehyde, methanol, acetone, acetonitrile, and hydrogen cyanide, *Geophys. Res. Lett.*, *26*, 1161-1164, 1999.

Lal, S., M. Naja, and A. Jayaraman, Ozone in the marine boundary layer over the tropical Indian Ocean, *J. Geophys. Res.*, *103*, 18907-18917, 1998.

Lelieveld, J., A. Bregman, H.A. Scheeren, J. Ström, K.S. Carslaw, H. Fischer, P.C. Siegmund, and F. Arnold, Chlorine activation and ozone destruction in the northern lowermost Stratosphere, *J. Geophys. Res.*, *104*, 8201, 1999.

Lelieveld, J., and F.J. Dentener, What controls tropospheric ozone ?, *J. Geophys. Res.*, *105*, 3531, 2000.

Lelieveld, J., et al., Large impact of Southeast Asian air pollution: Results from the Indian Ocean Experiment, *J. Geophys. Res.*, this issue, 2001.

Lindinger, W., A. Hansel, and A. Jordan, On-line monitoring of volatile organic compounds at pptv levels by means of Proton-Transfer-Reaction Mass Spectrometry (PTR-MS). Medical Applications, food control and environmental research, *Int. J. Mass Spec. Ion Proc.*, *173*, 191-241, 1998.

Lobert, J.M., V. Ramanathan, J. Prospero, and A. Majeed, Kaashidhoo Climate Observatory (KCO): A new site for observing long-term changes in the tropical Indian Ocean, *J. Geophys. Res.*, this issue, 2001.

McKeen, S.A., T. Gierczak, J.B. Burkholder, P.O. Wennberg, T.F. Hanisco, E.R. Keim, R.-S. Gao, S.C. Liu, A.R. Ravishankara, and D.W. Fahey, The photochemistry of acetone in the upper troposphere: A source of odd-hydrogen radicals, *Geophys. Res. Lett.*, *24*, 3177-3180, 1997.

Olivier, J.G.J., et al., Description of EDGAR version 2.0: a set of global emission inventories of greenhouse gases and ozone depleting substances for all anthropogenic and most natural sources on a per country basis on $1^{\circ}\times1^{\circ}$ grid, *RIVM report 771060 002 and TNO MEP report R96/199*, National Institute for Public Health and the Environment, Bilthoven, the Netherlands, 1996.

Rhoads, K.P., P. Kelley, R.R. Dickerson, T.P. Carsey, M. Farmer, D.L. Savoie, and J.M. Prospero, Composition of the troposphere over the Indian Ocean during the monsoonal transition, *J. Geophys. Res.*, *102*, 18981-18995, 1997.

Satheesh, S.K. and V. Ramanathan, Large differences in tropical aerosol forcing at the top of the atmosphere and the Earth's surface, *Nature*, *405*, 60 (2000).

Scheele, M.P., P.C. Siegmund, and P.F.J. van Velthoven, Sensitivity of trajectories to data resolution and its dependence on the starting point: in or outside a tropopause fold, *Meteorol. Appl.*, *3*, 267-273, 1996.

Scheeren, H.A., J. Lelieveld, J.A. de Gouw, C. van der Veen, H. Fischer, Methyl chloride in polluted air during INDOEX, *J. Geophys. Res*, this issue, 2001.

Singh, H.B., D. O'Hara, D . Herlth, W. Sachse, D.R. Blake, J.D. Bradshaw, M. Kanakidou, and P.J. Crutzen, Acetone in the atmosphere: Distribution, sources and sinks, *J. Geophys. Res.*, *99*, 1805-1819, 1994.

Smit, H.G.J., D. Kley, R. Cremer, and M. Zachariasse, Large scale distribution of ozone and humidity over the Indian Ocean between 15°S and 15°N during INDOEX: Evidence for large scale outflow of Indian pollution, *J. Geophys. Res*, this issue, 2001.

Stohl, A., L. Haimberger, M.P. Scheele, H. Wernli, An intercomparison of results from three trajectory models, *Meteorol. Appl.*, accepted, 2000.

Veldt, C., J.J.M. Berdowski, GEIA-note on the combustion of biomass fuels (emission factors for CO, CH_4 and NMVOC), *TNO-report R94/218*, TNO Institute of Environmental Sciences, Delft, the Netherlands, 1995.

Verver, G., M. Zachariasse, D. Sikka, and G. Stossmeister, Overview of the meteorological conditions and atmospheric transport processes during the INDOEX IFP 1999, *J. Geophys. Res*, this issue, 2001.

Wienhold, F.G., H. Fischer, P. Hoor, V. Wagner, R. Konigstedt, G.W. harris, J. Anders, R. Grisar, M. Knothe, W.J. Riedel, Tristar – a tracer in situ TDLAS for atmospheric research, *Appl. Phys. B: Lasers and Optics*, *67*, 411-417, 1998.

Williams, J., H. Fischer, S. Wong, P.J. Crutzen, R. Scheele, M. Zachariasse, P. van Velthoven, H.A. Scheeren and J. Lelieveld, Vertical profiles of CO, O_3 and relative humidity, North and south of the ITCZ over the Indian Ocean during the winter Monsoon: evidence of two mechanisms for the influx of ozone rich air to the tropical upper troposphere and of interhemispheric exchange, *J. Geophys. Res.*, this issue, 2001.

Warneke, C., J. A. de Gouw, H. A. Scheeren, A. T. J. de Laat, J. Lelieveld, S. Wong, J. Williams, H. Fischer, M.G. Lawrence, and P.J. Crutzen, Hydroxyl radical concentration in the boundary layer over the Indian Ocean estimated from an airborne Lagrangian experiment in March 1999 during INDOEX, *J. Geophys. Res.*, this issue, 2001.

Zachariasse, M., H.G.J. Smit, P.F.J. van Velthoven, and R. Cremer Stratosphere-troposphere exchange over the Indian Ocean during INDOEX 1999, *J. Geophys. Res.*, this issue, 2001.

Table 1: Overview of the trace gas measurements performed from the Citation during INDOEX.

Measurement	Technique	P.I.	Institution
O_3	Chemiluminescence	Scheeren	IMAU
CO, N_2O, CH_4	TD-LAS [a]	Fischer	MPI Mainz
Acetone, acetonitrile	PTR-MS [b]	De Gouw	IMAU
NMHCs, halocarbons	GC-FID [c], GC-ECD [d]	Scheeren	IMAU
CO_2	IR absorption	Fischer	MPI Mainz
NO, NO_2	Chemiluminescence	Helas	MPI Mainz

(a) TD-LAS = tunable diode laser absorption spectroscopy (*Wienhold et al.*, 1998).

(b) PTR-MS = proton-transfer-reaction mass spectrometry (*Lindinger et al.*, 1998).

(c) GC-FID = gas chromatography with flame ionization detection (*Scheeren et al.*, 2001).

(d) GC-ECD = gas chromatography with electron capture detection (*Scheeren et al.*, 2001).

(e) Institute for marine and atmospheric research, Utrecht University, the Netherlands.

(f) Max Planck Institute for Chemistry, Mainz, Germany.

Table 2: Average mixing ratios of trace compounds observed during INDOEX. The ozone, CO and acetone mixing ratios are in ppbv, the other values in pptv. The error bars indicate the standard deviation.

	0-3 km		3-8 km		8-13 km	
Compound	Feb	Mar	Feb	Mar	Feb	Mar
Ozone	13±5	12±4	23±7	17±5	29±11	21±4
CO	220±40	150±30	130±40	100±12	110±20	113±18
Acetone	2.2±0.3	1.4±0.4	0.9±0.2	0.6±0.4	0.76±0.13	0.5±0.2
Acetonitrile	330±50	260±50	170±70	130±40	110±50	80±30
Ethane	900±300	530±190	670±160	520±190	540±90	480±110
Propane	60±40	30±30	49±14	40±30	62±17	40±20
Acetylene	330±190	120±80	150±140	60±40	130±30	100±40
Benzene	110±40	50±30	40±40	18±9	50±15	32±13
Methyl chloride	900±80	780±70	770±80	720±40	770±20	740±30

Table 3: Emission factors of NMHCs measured during INDOEX onboard the Citation.

Compound	k_{OH} (cm^3 $molecule^{-1}$ s^{-1})	ΔNMHC/ΔCO (pptv $ppbv^{-1}$)	Literature (pptv $ppbv^{-1}$)	Age corrected (pptv $ppbv^{-1}$)
Acetone	2.2×10^{-13} (a)	14.0±1.8	25 (20-30) (d)	
Acetonitrile	2.2×10^{-14} (a)	1.1±0.4	1.3 (0.4-2.5) (e)	
Ethane	2.5×10^{-13} (a)	5.8±0.3	9.3 (6-12) (c)	7.2±0.4
Propane	1.1×10^{-12} (a)	0.4±0.1	1.7 (1-3) (c)	
Acetylene	9.0×10^{-13} (a)	3.3±0.2	7.9 (4-15) (c)	8.7±0.5
Benzene	1.23×10^{-12} (b)	0.95±0.05	4.2 (3-5) (c)	2.3±0.3
Methyl chloride	4.2×10^{-14} (a)	1.7±0.2	???	

(a) *Atkinson et al.*, 1997.

(b) *Atkinson*, 1994.

(c) *Veldt and Berdowski*, 1995.

(d) *Singh et al.*, 1994.

(e) *Holzinger et al.*, 1999.

Figure captions

Figure 1: Indian Ocean region studied during the Intensive Field Phase of INDOEX by the Citation aircraft. Flight Tracks are indicated by the gray lines.

Figure 2: Histogram of the wind direction during the Citation flights. The y-axis gives the number of times the wind direction of the sampled air mass was within a certain interval.

Figure 3: Ten-day back-trajectories of the air masses sampled below an altitude of 3 km. One trajectory per level flight track is shown.

Figure 4: Latitude dependence of the ozone mixing ratio in three different altitude ranges measured during all the Citation flights. The data are averaged values for all the level parts of the flights, and the error bars are given by the standard deviation. Solid symbols are data from February, open symbols from March 1999.

Figure 5: Altitude profile of the ozone mixing ratio measured during the Citation flights (solid symbols: February; open symbols: March 1999).

Figure 6: Latitude dependence of the CO mixing ratio measured with TD-LAS on the Citation (solid symbols: February; open symbols: March 1999). The data are averaged values for all the level parts of the flights, and the error bars are given by the standard deviation.

Figure 7: Altitude dependence of the measured CO mixing ratio (solid symbols: February; open symbols: March 1999).

Figure 8: Altitude dependence of the acetone (CH_3COCH_3) and acetonitrile (CH_3CN) volume mixing ratios measured with PTR-MS on the Citation (solid symbols: February; open symbols: March 1999). The data are averaged values for all the level parts of the flights, and the error bars are given by the standard deviation.

Figure 9: Latitude dependence of the mixing ratios of ethane, acetylene and benzene in the 0-3 km altitude range.

Figure 10: Average trace gas mixing ratios measured in air masses carrying polluted air from three different source areas: BB is Bay of Bengal, AS is Arabian Sea, and SH is Southern Hemisphere. The error bars show the standard deviation.

Figure 11: Correlation between the mixing ratios of acetone and CO measured during INDOEX. The data are averaged values for all the level flight tracks and the error bars are the standard deviation in the individual measurement points.

Figure 12: Correlation between the mixing ratios of acetonitrile and CO measured during INDOEX. The data are averaged values for all the level flight tracks and the error bars are the standard deviation in the individual measurement points.

Figure 13: Correlation between mixing ratios of CO and a number of trace gases measured from gas samples taken during INDOEX onboard the Citation. The CO data are averaged values for the level flight tracks during which the gas canister were sampled.

Figure 14: Determination of the age of the air masses sampled by the Citation. The plot shows the comparison between the age determined from the acetylene/benzene ratio on the one hand, and the benzene/ethane ratio on the other hand.

Figure 15: Estimated age of the sampled air masses below 3 km altitude vs. the latitude.

Figure 16: Altitude profile of the estimated age of the sampled air masses.

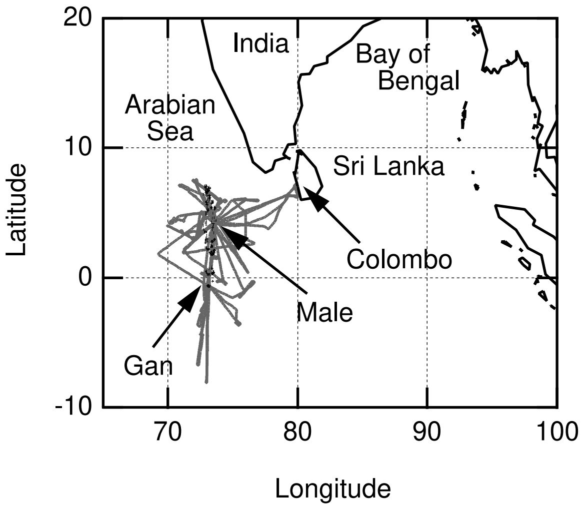
India
Bay of
Bengal
Arabian
Sea
Sri Lanka
Colombo
Male
Gan
Latitude
Longitude
20
10
0
-10
70
80
90
100

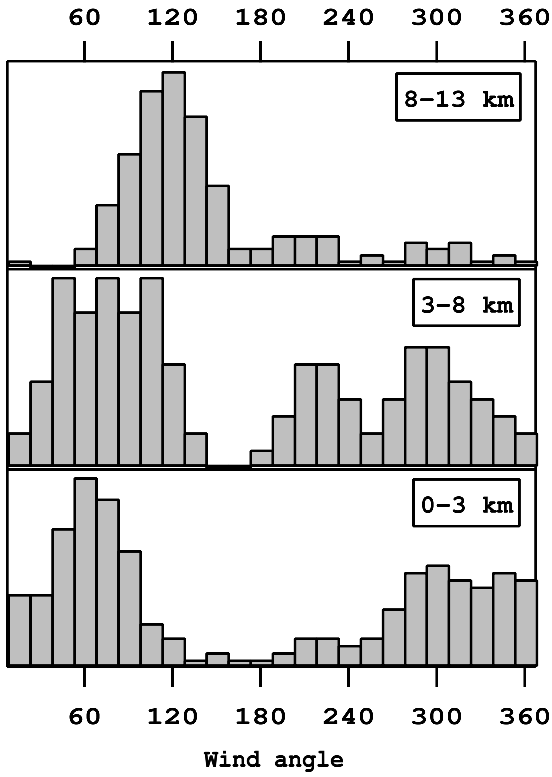
60
120
180
240
300
360
8–13 km
3–8 km
0–3 km
60
120
180
240
300
360
Wind angle

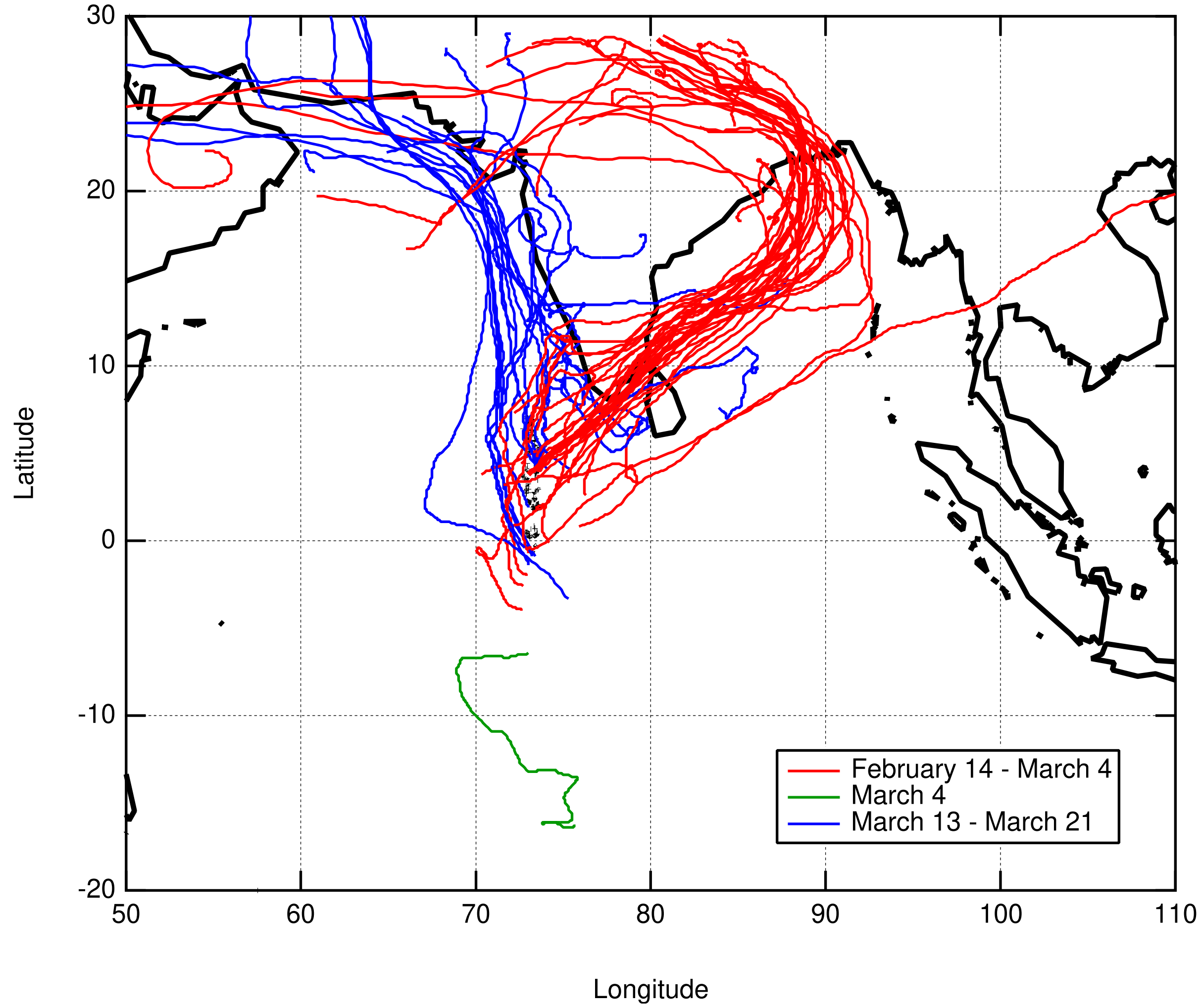
30
20
10
0
-10
-20
Latitude
50
60
70
80
90
100
110
Longitude
February 14 - March 4
March 4
March 13 - March 21

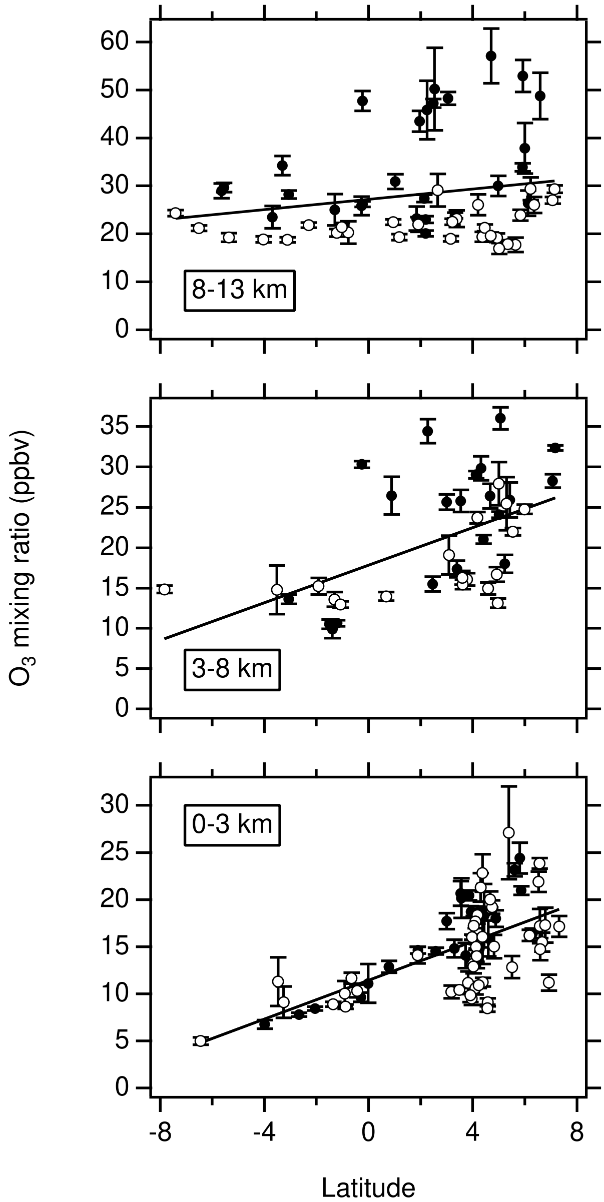
8-13 km
3-8 km
0-3 km
O_3 mixing ratio (ppbv)
Latitude
60
50
40
30
20
10
0
35
30
25
20
15
10
5
0
30
25
20
15
10
5
0
-8
-4
0
4
8

Figure 5 **de Gouw et al.**

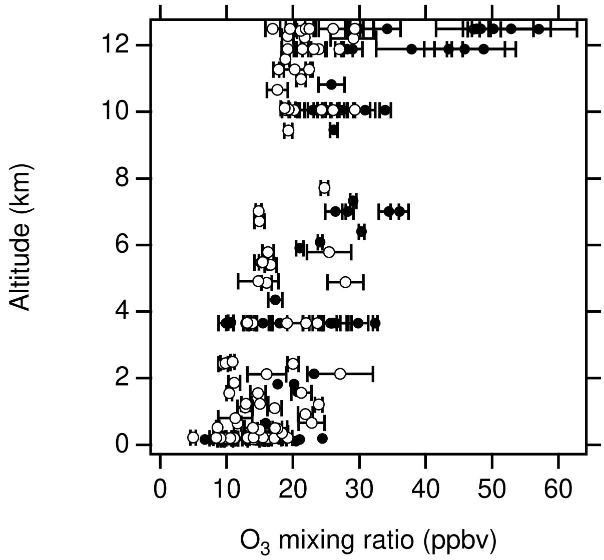

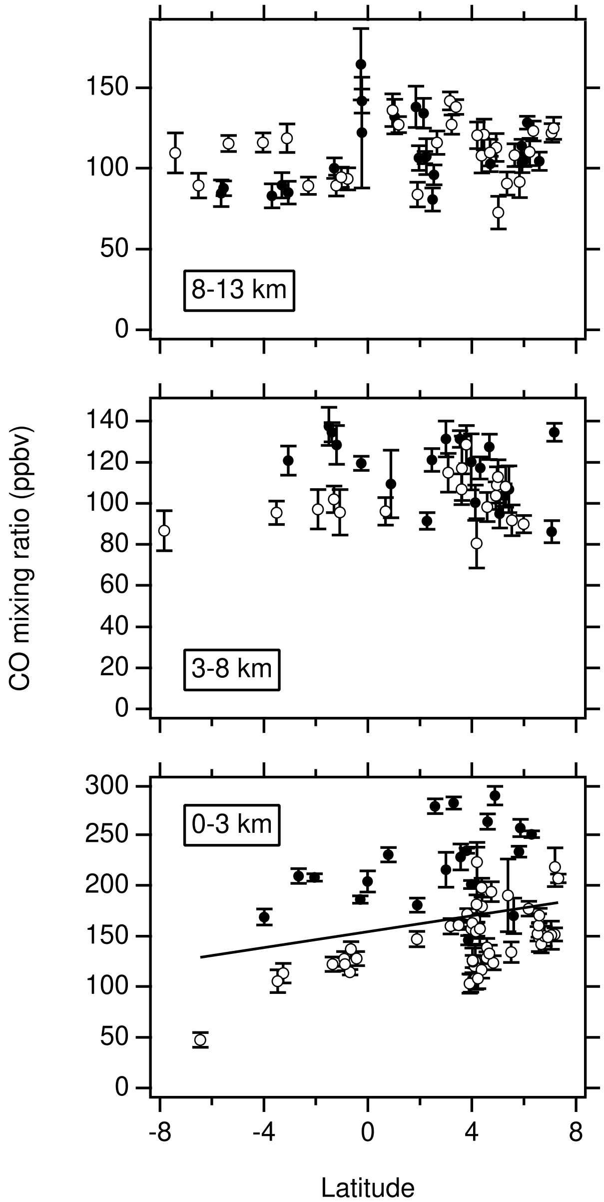

150
100
50
0
8-13 km
140
120
100
80
60
40
20
0
3-8 km
CO mixing ratio (ppbv)
300
250
200
150
100
50
0
0-3 km
-8
-4
0
4
8
Latitude

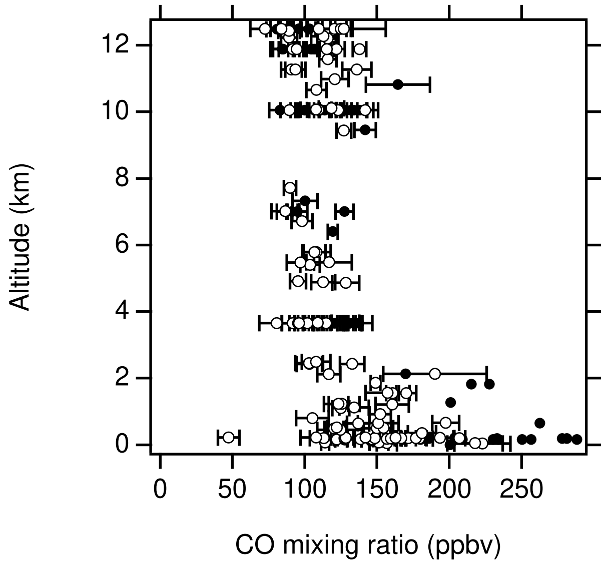

Altitude (km)
12
10
8
6
4
2
0
0
50
100
150
200
250
CO mixing ratio (ppbv)

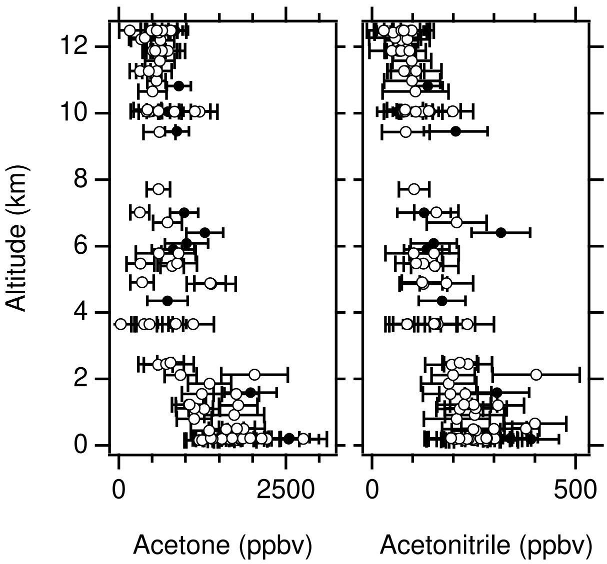
Altitude (km)
0
2
4
6
8
10
12
0
2500
Acetone (ppbv)
0
500
Acetonitrile (ppbv)

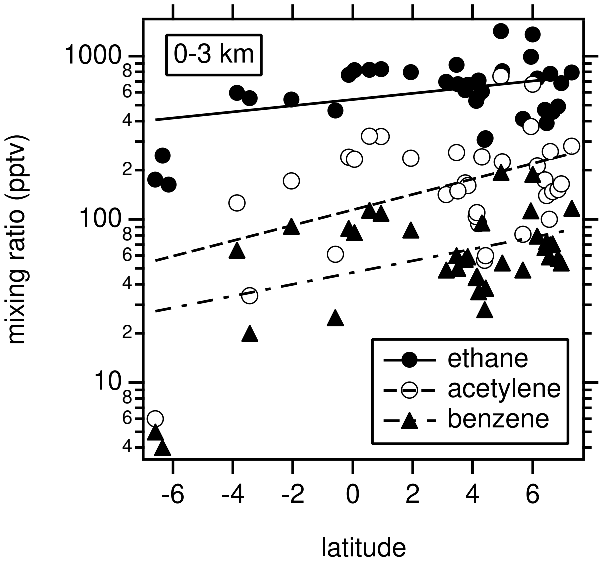
0-3 km
1000
100
10
mixing ratio (pptv)
-6 -4 -2 0 2 4 6
latitude
ethane
acetylene
benzene

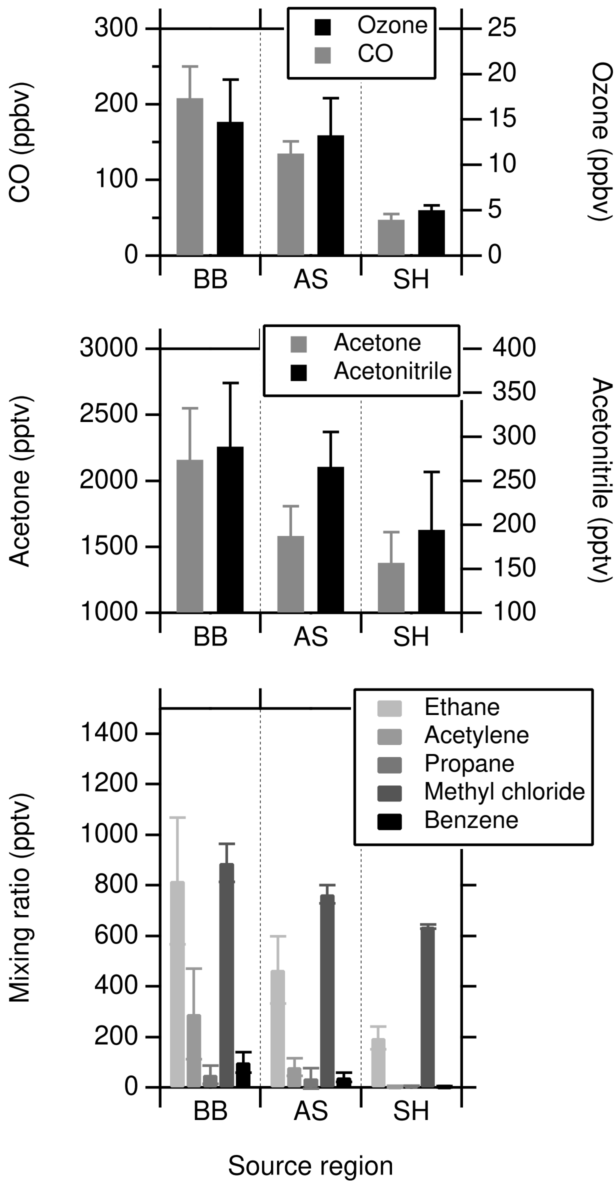

Ozone
CO
CO (ppbv)
Ozone (ppbv)
300
200
100
0
25
20
15
10
5
0
BB
AS
SH
Acetone
Acetonitrile
Acetone (pptv)
Acetonitrile (pptv)
3000
2500
2000
1500
1000
400
350
300
250
200
150
100
Ethane
Acetylene
Propane
Methyl chloride
Benzene
Mixing ratio (pptv)
1400
1200
1000
800
600
400
200
0
Source region

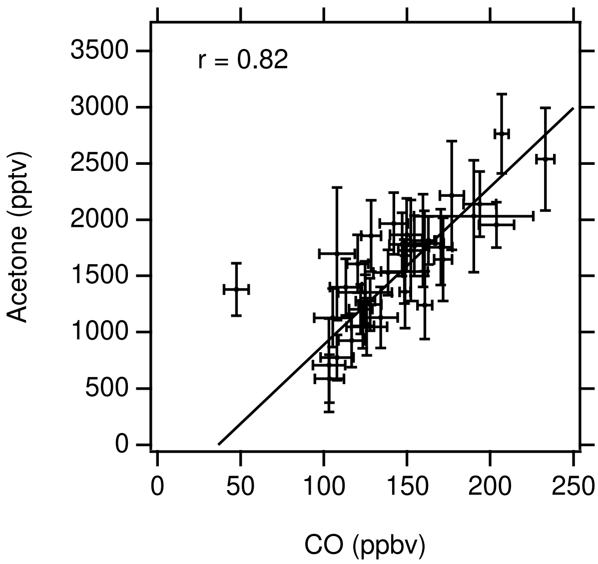
r = 0.82
3500
3000
2500
2000
1500
1000
500
0
Acetone (pptv)
0
50
100
150
200
250
CO (ppbv)

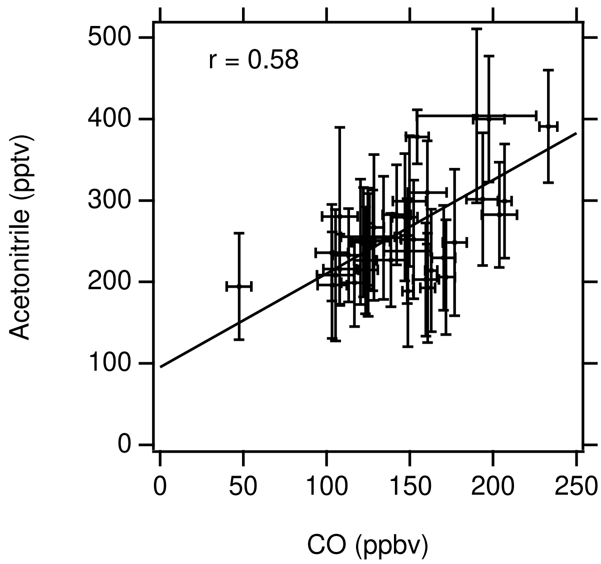
r = 0.58
Acetonitrile (pptv)
CO (ppbv)
0
100
200
300
400
500
0
50
100
150
200
250

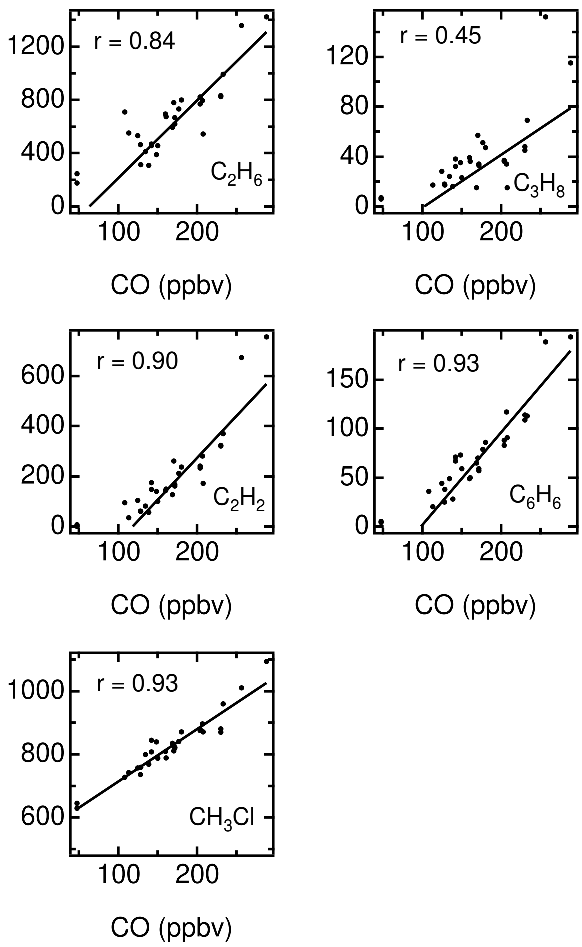
r = 0.84
1200
800
400
0
100
200
C_2H_6
CO (ppbv)
r = 0.45
120
80
40
0
100
200
C_3H_8
CO (ppbv)
r = 0.90
600
400
200
0
100
200
C_2H_2
CO (ppbv)
r = 0.93
150
100
50
0
100
200
C_6H_6
CO (ppbv)
r = 0.93
1000
800
600
100
200
CH_3Cl
CO (ppbv)

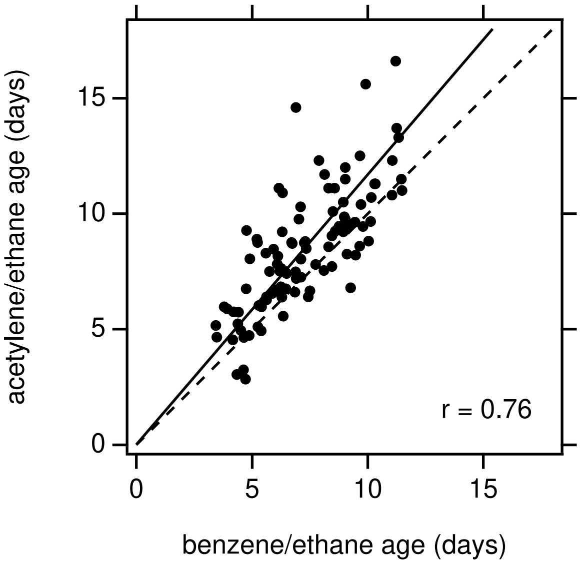

acetylene/ethane age (days)
benzene/ethane age (days)
r = 0.76
0
5
10
15

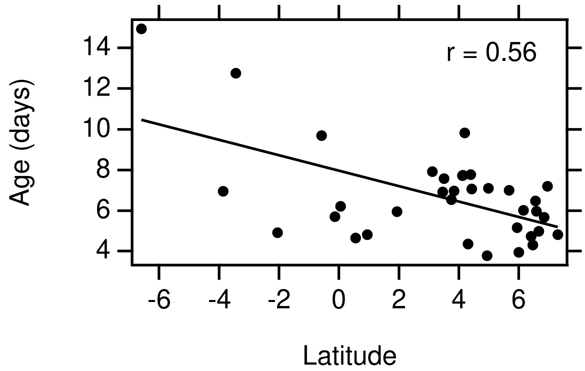
r = 0.56
Age (days)
14
12
10
8
6
4
-6
-4
-2
0
2
4
6
Latitude

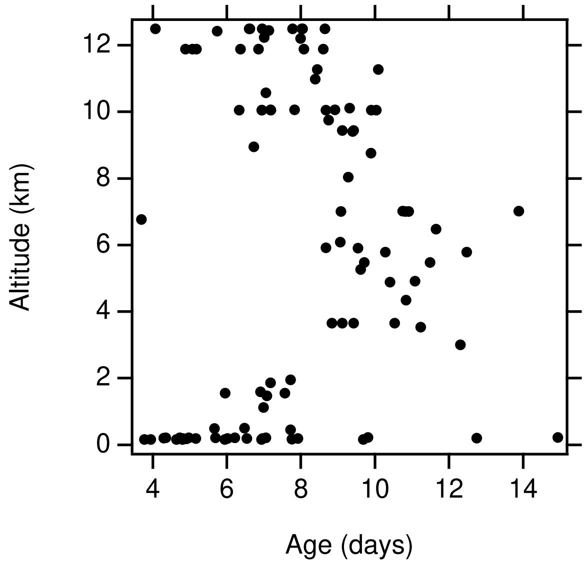
Altitude (km)
Age (days)
0
2
4
6
8
10
12
4
6
8
10
12
14